Quantum Electronics **49** (2) 157–161 (2019)

LASER APPLICATIONS AND OTHER TOPICS IN QUANTUM ELECTRONICS https://doi.org/10.1070/QEL16819

Measurements of water molecule isotopomer concentrations in a discharge of inert gas with addition of H_2O and D_2 vapours by the method of external-cavity diode laser spectroscopy

A.V. Bernatskiy, V.V. Lagunov, V.N. Ochkin

Abstract. **Discharge plasma in inert gases with added water vapours and deuterium is studied by using the optimised diode laser spectroscopy with an external cavity. Formation of a spectrally dense grid of cavity transverse mode eigenfrequencies allows one to determine the parameters of Doppler broadening for absorption lines, a kinetic temperature of molecules, and their statistical sums. By using these parameters and the value of an absorption coefficient, correlations of concentrations are found for H_2O and HDO isotopomers at various ratios of plasma-forming gas components. An important contribution of initial gas molecules adsorbed on walls into the formation of plasma composition is stressed. It is found that the ratio of H_2O and HDO concentrations is the same at various ratios of H_2O and D_2 concentrations in plasma-forming gases and is constant during the discharge burning process.**

Keywords: *absorption spectroscopy, diode laser, external cavity, gas discharge, isotopic modifications of water molecule, plasmochemistry.*

1. Introduction

In the last approximately 20 years, high-resolution absorption spectroscopy methods has been developing with the employment of diode lasers for detecting trace concentrations of particles and their isotopic modification [1]. Content measurements for such particles is important in many applications including atmosphere content monitoring [2, 3], gas flow parameters [4], and medical diagnosis [5]. A relative content of isotopomers H_2O and HDO was also studied in [6–8]. However, almost all measurements are taken in the conditions of thermodynamic equilibrium of studied media. For non-equilibrium systems, it is actually impossible to use results obtained.

Presently, in view of preparing to the ITER start-up, it is necessary to control plasma impurities, first of all, water molecules, which penetrate the first multi-element reactor wall from a cooling circuit [9]. Engineering complexity of the installation and restricted access to plasma make non-contact methods preferable. Attempts were made to use diode laser spectroscopy by placing a spectrometer directly into a chamber of a Tore Supra reactor [10]. However, even in this 'cold' regime the required sensitivity to H_2O molecules implied in the reactor project [9] has not been achieved. Thus, a particular attention in the literature was paid to optical emission methods. The required sensitivity to a water vapour flow passed to plasma (10^{-7} Pa m^3 s^{-1}) was obtained by using specially developed emission optical actinometric methods [11–14]. Nevertheless, in this case such methods are indirect because water molecules, H_2O, are detected by glow of their single- and two-atom decay fragments (OH, H, O, ...) and base actinometers (Ar, Xe) with the following calculations of the rates of plasmochemical reactions [12]. Such a scheme is acceptable if the plasma-forming gas consists of inert atoms with water vapours. This is also confirmed by direct laser absorption measurements of H_2O concentration [15].

Note that presently laser methods are being actively used for studying plasma objects and discharge processes [16]. However, some problems of optical diagnostics of impurities in near-wall low-temperature plasma of fusion reactors are still open. In particular, the deuterium molecule D_2 is a natural component in a plasma-forming gas. Due to similar structures, initial H_2O molecules and, possibly, (not observed yet) HDO molecules synthesised in deuterated plasma may participate in competing reactions [17]; however, there are no direct measurements of a concentration ratio for isotopomers H_2O and HDO in a discharge, which hinders further analysis. In the present work, such measurements are performed in gas discharge plasma by using diode lasers.

Our study is aimed at simultaneous measurement of H_2O and HDO isotopomer concentrations in a discharge and determining the concentration ratio.

2. Measurement scheme

An experimental setup is shown schematically in Fig. 1. A dc discharge (2 mA) burns in a water-cooled quartz tube (*3*). The discharge length along the tube axis between electrodes (*7*) and (*9*) was 40 cm, the total tube length was 45 cm, and its internal diameter was 2 cm. The system for gas evacuation and puffing is connected to socket (*6*); the tube was evacuated to a pressure of 10^{-4} Torr and filled with an H_2O-D_2-He mixture at various component ratios and the sum pressure of up to 1 Torr, which was controlled by a Pfeiffer TPR250 sensor. Measurements were taken in a positive column of the glow discharge; the electrodes were connected to side contacts. Three similar electrodes controlled the electric field strength in a positive column. Alternate connection of a high-voltage source to electrode pairs (*7*) and (*8*), (*7*) and (*9*), and (*8*) and (*9*) allows one to exclude a cathode drop from the voltage across the discharge.

A.V. Bernatskiy, V.V. Lagunov, V.N. Ochkin P.N. Lebedev Physical Institute, Russian Academy of Sciences, Leninsky prosp. 53, 119991 Moscow, Russia; e-mail: ochkinvn@lebedev.ru, lagunoww@yandex.ru, bernatskiyav@lebedev.ru

Received 17 September 2018; revision received 9 November 2018
Kvantovaya Elektronika **49** (2) 157–161 (2019)
Translated by N.A. Raspopov

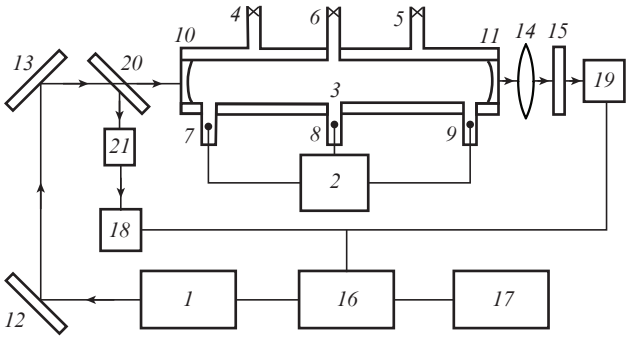

Figure 1. Schematic of the experimental setup:
(*1*) diode laser; (*2*) high-voltage power supply; (*3*) discharge tube; (*4*, *5*) cooling water sockets; (*6*) socket for connecting vacuum and gas puffing systems; (*7–9*) electrodes; (*10*, *11*) cavity mirrors; (*12*, *13*) foldable mirrors for varying the angle of radiation input into a cavity; (*14*) lens; (*15*) filter; (*16*) ADC/DAC; (*17*) computer; (*18*, *19*) radiation detectors; (*20*) beam splitter; (*21*) Fabry–Perot standard.

A DM-1392 diode laser (Elbana Photonics) with a radiation power of up to 8 mW near $\lambda = 1392$ nm, linewidth of 2 MHz ($\sim 10^{-4}$ cm^{-1}) and frequency tuning range of 2 cm^{-1} (at a fixed temperature of 304 K) was used in experiments. The frequency was tuned by the following modulation of the pump current: first, a time interval of duration 0.5 ms with zero current, which determines the time interval between repeating pulses. Then a constant-current (30 mA) plateau is formed with a duration of 1.5 ms for obtaining a threshold current and stabilising the initial frequency. After that, the current linearly increases from 30 mA to 115 mA during a time interval of ~3 ms, which provides frequency tuning. Finally, the current drops to zero again. The current is controlled discretely with a time step of 1–1.5 ms.

The optical cavity is formed by the tuning units mounted at tube ends with two similar spherical mirrors (*10*) and (*11*). Reflection coefficients of the mirrors were 99.98% (data from Layertec) at $\lambda = 1392$ nm, and the mirror radii were 1 m. Foldable mirrors (*12*) and (*13*) control the angle of emission input relative to the cavity axis.

Parasitic absorption by molecules H_2O and other background molecules in atmospheric air in the path outside the discharge chamber was excluded by controlling a base line. For this purpose, part of the laser beam split by beam splitter (*20*) passed to detector (*18*). Here, the path length in open atmosphere from laser (*1*) to detector (*18*) is equal to the total length of open trace segments form laser (*1*) to ThorLabs PDA10CS-EC detector (*19*), which detects the radiation passed through the cavity and collected by lens (*14*). The degree of suppressing parasitic absorption was verified at the evacuated discharge tube. Interference filter (*15*) separated the laser radiation from the plasma background glow passed through the cavity. In addition, interferometer (*21*) was placed in the base line channel for reproducing the frequency scale in the process of laser frequency tuning. Frequency tuning and the base line were controlled by the method described in [3]. Computer (*17*) and a PCI-6120 ADC/DAC interface card (National Instruments) provided data acquisition and control of the laser.

3. Measurement method

Presently, there are many methods of using external cavities in high-sensitivity absorption laser spectroscopy. In all cases (CRDS, ICOS, etc.), a common feature is increasing the effective cavity optical length. The maximal cavity length and Q-factor are obtained in the axial scheme of operation in the fundamental longitudinal mode with minimal diffraction losses, which, in turn, implies high cavity stability. Stability requirements may be softer in a case of simultaneous operation at several transverse modes, for example, when the input radiation beam is shifted relative to the cavity axis (non-axial scheme) [1]. In this case, the Q-factor and intensity of passed radiation are lower; however, there may be a compromise between the sensitivity and stability of such radiation. In addition, the problem considered is specific in that we deal with a low-pressure object possessing narrow (Doppler) absorption line profiles comparable to the separation between cavity axial modes.

In our experiments, the angle between the beam and cavity axes determined by mirrors (*12*) and (*13*) was less than one degree. Before measurements, a radiation decay time τ was determined in the axial system configuration by the rear edge of a laser pulse. This time is 11.5 ± 0.5 μs and corresponds to the effective reflection coefficient $R_{\text{eff}} = (R_{10}R_{11})^{1/2} = 0.99987 \pm 0.00005$ of mirrors (*10*) and (*11*), which is close to data of producer (Layertec). In the non-axial scheme employed, the decay time τ^* was 10.5 ± 0.5 μs, which is related to additional diffraction losses that can be formally included into the efficient mirror reflection coefficients: $R^*_{\text{eff}} = 0.99986 \pm 0.00005$. This corresponds to the optical path length $L = \tau^* c = 3150$ m.

Particle concentration was found by using the Bouguer–Lambert–Beer law

$$I(\nu) = I_0(\nu)\exp[-\alpha_{\text{low-up}}(\nu)L], \tag{1}$$

where I_0 and I are experimentally measured intensities of radiation entering the cavity and passed through it, respectively; and $\alpha_{\text{low-up}}$ is the absorption index for a transition between low and upper molecule levels. The concentration was conventionally calculated by using the absorption cross section $\sigma_{\text{low-up}}$ (cm^2). If the particles are two-level and all reside at the lower level (that is, N equals to N_{low}) we have $\alpha_{\text{low-up}}(\nu) = \sigma_{\text{low-up}}(\nu)N$. Modern molecular spectroscopy databases (for example, HITRAN [18] and GEISA [19]) utilise the normalised form-factor of absorption profile $\varphi(\nu)$ (cm) and the absorption line strength $S_{\text{low-up}}$ (cm mol^{-1}) at a low-up transition, which are related to the cross section as follows:

$$\sigma_{\text{low-up}}(\nu) = S_{\text{low-up}}\varphi(\nu), \tag{2}$$

$$\int_0^\infty \varphi(\nu)\,\mathrm{d}\nu = 1. \tag{3}$$

For two-level particles, their concentration at a lower level is determined by the expression

$$N_{\text{low}} = \frac{1}{LS_{\text{low-up}}\varphi(\nu)}\ln\frac{I_0(\nu)}{I(\nu)}. \tag{4}$$

However, since molecules are multilevel systems, calculation of the total concentration requires taking into account the statistical sum

$$Q = \frac{1}{N}\sum_k g_k N_k, \tag{5}$$

where g_k and N_k are the statistical weight and population of the kth level including the lower one, respectively. In thermodynamic equilibrium, the molecule distribution over rotation, vibration, and electron levels is determined by temperature T and molecular constants. In these conditions, the values of $Q(T)$ in the databases mentioned above (see also [20]) are given for a wide temperature range (up to 3000 K).

Note that HITRAN presents values for $S_{\mathrm{low-up}}$ taking into account abundance of particular isotopic modifications; this fact was used in the calculations. Databases present $S_{\mathrm{low-up}}$ for the temperature $T_{\mathrm{ref}} = 296$ K. For an arbitrary temperature and each particular isotopomer, we have

$$S_{\mathrm{low-up}}(T) = S_{\mathrm{low-up}}(T_{\mathrm{ref}})\frac{Q(T_{\mathrm{ref}})}{Q(T)} \times \frac{\exp\left(-\frac{hcE_{\mathrm{low}}}{k_{\mathrm{B}}T}\right)\left[1-\exp\left(-\frac{hc\nu_{\mathrm{low-up}}}{k_{\mathrm{B}}T}\right)\right]}{\exp\left(-\frac{hcE_{\mathrm{low}}}{k_{\mathrm{B}}T_{\mathrm{ref}}}\right)\left[1-\exp\left(-\frac{hc\nu_{\mathrm{low-up}}}{k_{\mathrm{B}}T_{\mathrm{ref}}}\right)\right]}. \quad (6)$$

Here, k_{B} is the Boltzmann constant; E_{low} is the low-level energy; and $\nu_{\mathrm{up-low}} = E_{\mathrm{up}} - E_{\mathrm{low}}$. If in formula (4) we use $S_{\mathrm{low-up}}$ (6) then, instead of N_{low} we obtain the total concentration N for a particular kind of molecules.

Conventionally, there is no thermodynamic equilibrium in a discharge plasma. However, in the conditions considered, we may assume that the system is in thermodynamic equilibrium to a good accuracy due to small rotational constants of molecules, fast vibrational relaxation in the presence of water molecules, and small population of excited electron levels [21]. For particles in ground electron states, deviations from the Maxwellian distribution are rather rare and the temperature of neutral gas at the considered low pressures can be obtained reliably from a Gaussian profile of Doppler absorption profile.

$$\varphi(\nu) = \varphi(\nu_0)\exp\left[-\frac{M}{2k_{\mathrm{B}}T}c^2\left(\frac{\nu-\nu_0}{\nu_0}\right)^2\right], \quad (7)$$

where M is the mass of molecule. In the range of laser radiation tuning, four HDO and three H_2O absorption lines are detected, which differ in the line strengths (Table 1, Fig. 2). This gives a possibility to use weaker lines at high molecule concentrations and stronger lines at low concentrations expanding in this way the dynamic range of measurements.

Table 1 presents statistical sums Q for gas temperature T_0 in the cell prior to switching on the discharge, and Table 2 presents temperatures measured and the corresponding values $Q(T)$ in a discharge for mixtures with various initial compositions. The temperatures from Table 2 correspond to the initial (~20 s) instant after switching on the discharge. As was shown in experiments, in first 10 min of discharge burning, temperature variations are negligible (within the inaccuracy given in Table 2).

Table 1. Characteristics of employed absorption lines.

Molecule	Frequency/ $\mathrm{cm^{-1}}$ [18, 19]	Line strength/ $\mathrm{cm\ mol^{-1}}$ [18, 19]	Transition [18, 19]	Q ($T_0 = 302 \pm 5$ K) [20]
HDO	7179.99	4.20×10^{-25}	P(4) (000–002)	890
	7180.34	3.05×10^{-25}	P(5) (000–002)	
	7180.74	4.53×10^{-26}	Q(4) (000–002)	
	7181.31	6.33×10^{-25}	P(4) (000–002)	
H_2O	7180.39	5.56×10^{-22}	P(4) (000–200)	180
	7180.61	2.95×10^{-23}	Q(9) (000–101)	
	7181.16	1.50×10^{-20}	P(3) (000–101)	

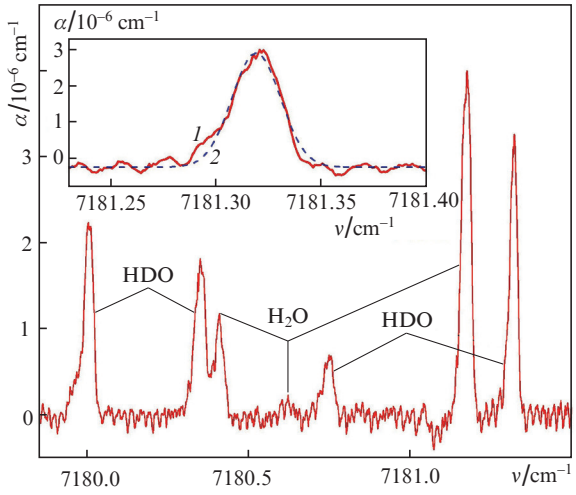

Figure 2. Absorption spectra of H_2O and HDO in a discharge in a He–D_2–H_2O mixture in the tuning range of laser radiation frequency. The inset shows the approximation of the HDO absorption line in the transition $\nu_0 = 7181.31$ $\mathrm{cm^{-1}}$ (*1*) by a Gaussian profile (*2*).

Table 2. Gas temperature in ~20 s after switching off the discharge and the corresponding values of Q for mixtures of various initial composition.

$n_0(H_2O)$/ 10^{14} $\mathrm{cm^{-3}}$	$n_0(D_2)$/ 10^{15} $\mathrm{cm^{-3}}$	T/K	Q (HDO)	Q (H_2O)
6.0	5.3	310 ± 5	927	187
4.4	3.6	315 ± 5	950	192
8.4	5.3	320 ± 5	973	196
8.4	1.8	335 ± 5	1042	210
9.6	1.8	340 ± 5	1066	215
4.8	1.8	345 ± 5	1094	220
8.8	3.6	355 ± 5	1138	229

Note: $n_0(H_2O)$ and $n_0(D_2)$ are the initial concentrations.

Spectra in Fig. 2 reveal no evident resonant properties of the cell. Issuing from this fact one can estimate the low limit for the mode spectral density in the non-axial scheme employed by the reciprocal value of the laser radiation frequency-tuning step. The tuning interval of 1 $\mathrm{cm^{-1}}$ corresponds to 1250 steps, that is, the mode separation of the scheme is at most 8×10^{-4} $\mathrm{cm^{-1}}$. This value defines the real spectral resolution determined by the discreteness of injection current control (at a slow instantaneous tuning it would be defined by the laser line width 10^{-4} $\mathrm{cm^{-1}}$).

4. Measurement results and discussion

In measurements, He–D_2–H_2O gas mixtures with various concentrations of H_2O and D_2 were introduced into the discharge tube at a fixed helium initial concentration $n_0(\mathrm{He}) = 8.5 \times 10^{15}$ $\mathrm{cm^{-3}}$. A typical absorption spectrum of the dis-

charge in a gas mixture with $n_0(D_2) = 5.3 \times 10^{15}$ cm^{-3} and $n_0(H_2O) = 8.4 \times 10^{14}$ cm^{-3} is shown in Fig. 2. In the inset, one can see an example approximation of an experimental absorption profile by a Gaussian profile (7). The best approximation corresponds to the gas temperature at the discharge axis $T = 320 \pm 5$ K. The experimental conditions only differed in the ratio of initial concentrations; the power deposited into the discharge varied weakly and was controlled by the field intensity in the discharge. In other conditions, the temperature values are presented in Table 2.

In Fig. 3 one can see measured time evolution of H_2O molecule concentration in a discharge at $n_0(D_2) = 1.8 \times 10^{15}$ cm^{-3} and various $n_0(H_2O)$. The measurement duration was 10 min. The time resolution was determined from the condition of providing a minimal error in data averaging while recording spectra. The Allan variance of the absorption index is shown in the insertion in Fig. 3. One can see that the optimal accuracy is reached at the averaging time of ~30 s, that is, in recording 2000–3000 spectra. The time intervals for data in Fig. 3 are 1 min. The sensitivity of absorption index measurements in the experimental conditions is $\pm 2 \times 10^{-7}$ cm^{-1}. The measurement dynamic range in the analytical spectral regions for H_2O is $3.4 \times 10^{11} - 2.1 \times 10^{15}$ cm^{-3} and for HDO it is $2.4 \times 10^{12} - 1.1 \times 10^{15}$ cm^{-3}. Low limits of the ranges are estimated from the Allan variance values and upper limits are derived from admissible errors at a high absorption and by using data from [22].

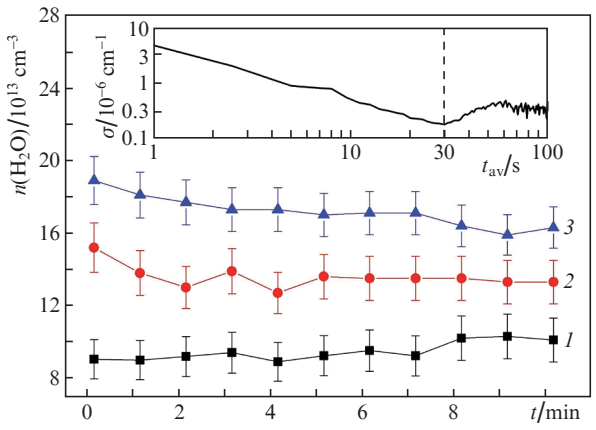

Figure 3. Time dependences of H_2O concentrations in a discharge at $n_0(D_2) = 1.8 \times 10^{15}$ cm^{-3} and $n_0(H_2O) = (1)\ 4.8 \times 10^{14}$, $(2)\ 8.0 \times 10^{14}$, and $(3)\ 9.6 \times 10^{14}$ cm^{-3}. The inset shows the Alan variance σ for the absorption index; t_{av} is the time of averaging.

Measurement results obtained for the water molecule concentration strongly differ from those obtained by actinometry in a hollow metal–ceramic cathode [12, 14]. H_2O molecules in a hollow cathode dissociate up to 95%–98%. In the present work, the H_2O concentration falls by at most 75%–85%. Seemingly, these differences are related to the specific feature discovered in our experiments.

After a long evacuation or 'training' the tube in a discharge, puffing of water vapours prior to switching on the discharge is accompanied by a fast pressure drop, which, obviously is related to molecule adsorption on tube walls. The values of $n_0(H_2O)$ presented above correspond to molecule concentrations in a gas phase at the initial instant after filling the tube. The 'stock' of captured molecules plays an important role in a total picture of chemical processes in a discharge. After switching on the discharge, part of molecules transfers to a gas phase. It may be related, for example, to collisions of helium atoms in metastable states with a wall. In addition, adsorbed molecules may react with active radicals H, O, D, OH and other. Although the dissociation remains fast, it is compensated by molecule transfer from walls to a gas phase. After the discharge switches on, a certain water concentration with participation of adsorbed molecules is rather quickly attained (in a time lapse of less than the measurement time of 30 s). This fact testifies that the main process of particle capture (release) on a surface is the physical adsorption (desorption) with Wan-der-Waals bond potentials, which needs a low activation energy as compared to a slow chemisorption where gas particles form strong chemical bonds with surface particles.

Time evolution of the HDO concentration in a discharge is shown in Fig. 4 at a fixed concentration $n_0(H_2O) = 8.4 \times 10^{14}$ cm^{-3} and various values of $n_0(D_2)$. Without discharge, HDO molecules are not detected, but those arise immediately after the discharge switches on. The weak (however, noticeable) tendency of heavy water concentration to fall is observed. The characteristic time of this process is dozens of minutes, therefore, it may be related to chemisorption.

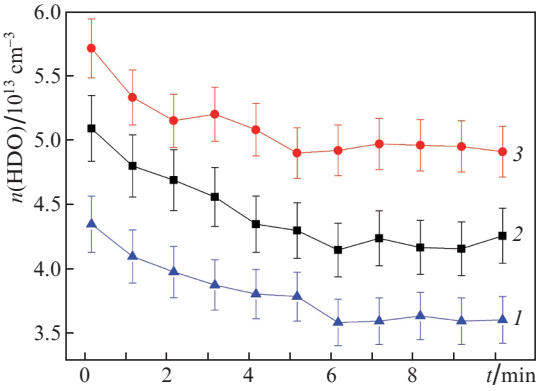

Figure 4. Time dependences of HDO molecule concentrations after switching on the discharge at $n_0(H_2O) = 8.4 \times 10^{14}$ cm^{-3} and $n_0(D_2) = (1)\ 1.8 \times 10^{15}$, $(2)\ 3.6 \times 10^{15}$, and $(3)\ 5.3 \times 10^{15}$ cm^{-3}.

The ratios $k = n(H_2O)/n(HDO)$ in a discharge were determined at various ratios of the initial D_2 and H_2O concentrations. It was found that the value of k is actually the same in all the cases considered ($k = 3 \pm 0.5$) and does not change in time. The corresponding results are presented in Fig. 5. We may assume there is a mechanism, which limits the number of H_2O molecules on a wall capable of overcoming a desorption barrier while interacting with D_2 molecules.

5. Conclusions

It is shown that water isotopomers H_2O and HDO in gas-discharge plasma can be directly simultaneously monitored by using the absorption diode laser spectroscopy with a single diode laser possessing a frequency tuning range of 2 cm^{-1} near $\lambda = 1392$ nm. In the case of combined strong and weak absorption lines, an external cavity with the mirrors mounted at the ends of a discharge tube provides the dynamic range of concentration measurements $3.4 \times 10^{11} - 2.1 \times 10^{15}$ cm^{-3} in an

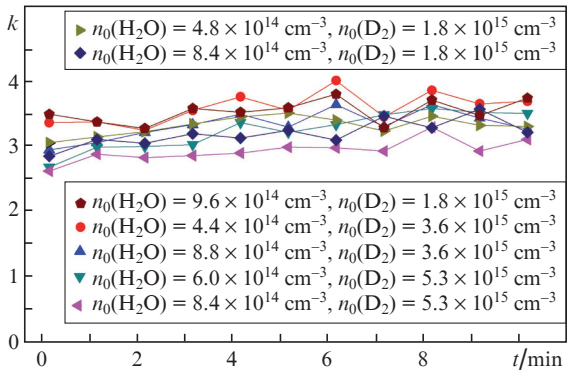

Figure 5. (Colour online) Time dependences of the ratio k of measured H_2O and HDO molecule concentrations in a discharge at various initial concentrations of H_2O and D_2 molecules.

analytical spectrum region of H_2O and 2.4×10^{12}–1.1×10^{15} cm^{-3} for HDO. With the mirrors arranged at a distance of 25 mm from a chemically active zone of a positive column at a current density of 1.6 kA cm^{-2}, degradation of mirror reflection coefficients near $\Delta R \approx 5 \times 10^{-5}$ was not observed for several months of experiments.

A quartz surface of the tube actively adsorbs water molecules, which then participate in reactions at the interface plasma-surface. The absolute concentrations of water molecules in both isotopic modifications depend on the initial concentrations of H_2O and D_2 molecules in the plasma-forming gas. However, the concentration ratio of H_2O and HDO is the same and remains constant in the process of discharge burning over the whole range of investigated compositions of plasma-forming gases. In view of this fact and observed rates of establishing stationary concentrations, one may assume that the capture of water by quartz surface is explained by physical adsorption and there is a mechanism, which limits the molecule desorption flow from the surface. This assumption requires further investigations.

Acknowledgements. The work was supported by the Russian Foundation for Basic Research (Grant No. 19-02-00540a).

References

1. Gagliardi G., Loock H.P. (Eds) *Cavity-Enhanced Spectroscopy and Sensing* (Berlin–Heidelberg: Springer, 2014); doi: 10.1007/978-3-642-40003-2.
2. Brazhnikov D.A., Nikolaev I.V., Ochkin V.N., et al. *Laser Phys.*, **19**, 1323 (2009); doi: 10.1134/S1054660X09060243.
3. Nikolaev I.V., Ochkin V.N., Peters G.S., et al. *Laser Phys.*, **23**, 035701 (2013); doi: 10.1088/1054-660X/23/3/035701.
4. Bolshov M.A., Kuritsyn Yu.A., Liger V.V., Mironenko V.R., Nadezhdinskii A.I., Ponurovskii Ya.Ya., Leonov S.B., Yarantsev D.A. *Quantum Electron.*, **45**, 377 (2015) [*Kvantovaya Electron.*, **45**, 377 (2015)]; doi: 10.1070/QE2015v045n04ABEH015590.
5. Zaitsev A.A., Nikolaev I.V., Ochkin V.N., Tskhai S.N. *Quantum Electron.*, **45**, 680 (2015) [*Kvantovaya Electron.*, **45**, 680 (2015)]; doi: 10.1070/QE2015v045n07ABEH015812.
6. Naumenko O.V., Voronin B.A., Mazzotti F., Tennyson J., Campargue A. *J. Mol. Spectrosc.*, **248**, 122 (2008).
7. Naumenko O.V., Beguier S., Leshchishina O.M., Campargue A. *J. Quantit. Spectrosc. Radiat. Transfer*, **111**, 36 (2010).
8. Shon W., Yim S.P., Lee L., Park H., Kim K.R., Chunga H., Lee C.K. *Fusion Eng. Des.*, **109-111**, 398 (2016).
9. ITER Final Design Report No. G 31 DDD 14 01.07.19 W 0.1, Section 3.1: Vacuum Pumping and Fuelling Stems.
10. Durocher Au., Bruno A., Chantant M., Gargiulo L., Gherman T., Hatchressian J.-C., et al. *Fusion Eng. Des.*, **88**, 1390 (2013).
11. Bernatskiy A.V., Ochkin V.N., Afonin O.N., Antipenkov A.B. *Plasma Phys. Rep.*, **41**, 705 (2015); doi: 10.1134/S1063780X15090032 [*Fiz. Plazmy*, **41**, 767 (2015); doi: 10.7868/S0367292115090036].
12. Bernatskiy A.V., Ochkin V.N., Kochetov I.V. *J. Phys. D: Appl. Phys.*, **49**, 395204 (2016); doi: 10.1088/0022-3727/49/39/395204.
13. Bernatskiy A.V., Ochkin V.N., Kochetov I.V. *Bull. Lebedev Phys. Inst.*, **44**, 147 (2017); doi: 10.3103/S1068335617050062 [*Kr. Soobshch. Fiz. FIAN*, **44**, 39 (2017)].
14. Bernatskiy A.V., Ochkin V.N. *Plasma Sources Sci. Technol.*, **26**, 015002 (2017); doi: 10.1088/0963-0252/26/1/015002.
15. Bernatskiy A.V., Lagunov V.V., Ochkin V.N., Tskhai S.N. *Laser Phys. Lett.*, **13**, 075702 (2016); doi: 10.1088/1612-2011/13/7/075702.
16. Parkevich E., Ivanenkov G., Medvedev M., Khirianova A., Selyukov A., Agafonov A.V., Mingaleev A., et al. *Plasma Sources Sci. Technol.*, **27**, 11LT01 (2018); doi: 10.1088/1361-6595/aaebdb.
17. Bernatskiy A.V., Kochetov I.V., Ochkin V.N. *Phys. Plasmas*, **25**, 083517 (2018); doi: 10.1063/1.5042839.
18. Gordon I.E. et al. *J. Quantit. Spectrosc. Radiat. Transfer*, **203**, 3 (2017).
19. Jacquinet-Husson N. et al. *J. Quantit. Spectrosc. Radiat. Transfer*, **109**, 1043 (2008).
20. http://spectra.iao.ru.
21. Ochkin V.N. *Spectroscopy of Low Temperature Plasma* (New York: Wiley-VCH, 2009).
22. Ochkin V.N. *Plasma Phys. Rep.*, **41**, 350 (2015); doi: 10.1134/S1063780X15040042 [*Fiz. Plazmy*, **41**, 381 (2015); doi: 10.7868/S0367292115040046].